Available online at www.sciencedirect.com
SCIENCE DIRECT®
International Journal of Thermal Sciences 44 (2005) 885–893
International Journal of Thermal Sciences
www.elsevier.com/locate/ijts

Experimental heat transfer on the windward surface of a perforated flat plate

E. Dorignac *, J.-J. Vullierme, M. Broussely, C. Foulon, M. Mokkadem

Laboratoire d'Etudes Thermiques, UMR CNRS 6608, Ecole Nationale Supérieure de Mécanique et d'Aérotechnique, 1, Av. Clément Ader BP 40109, 86961 Futuroscope Chasseneuil cedex, France

Received 20 April 2004; received in revised form 28 October 2004; accepted 30 November 2004

Available online 7 April 2005

Abstract

Two techniques are described in this paper to determine convective transfer on a multiperforated plate; the perforations diameter can be small or large (from 1 millimeter to 1 centimeter). This study reports on heat transfer due to the air flow before it goes through the perforations. These perforations are perpendicular to the wall. For a large range of perforations spacings, an empirical relation is proposed for heat exchange at the windward surface of a perforated flat plate.

Keywords: Film cooling; Windward surface; Forced convection; Infrared thermography; Correlation

1. Introduction

The increase of flame temperatures inside combustion chambers constrains aircraft and power generation gas turbine designers to set up new cooling schemes for the most exposed parts. Once the thrust has increased and the emission gases have dropped the melting point temperature of the turbine components and combustion chamber have been exceeded. As technologies had to be adapted to these extreme heat levels, the cooling flow around the external face of the combustion chamber had to be replaced by a full coverage film-cooling. A secondary flow derived from the compressor is injected through holes and creates a cooling film between the hot gases and either the internal face of the chamber or the turbine blades surface.

An important role is played by numerical studies to design cooling schemes and predict thermal stresses. These models need experimental results and heat transfer correlations for different geometrical configurations. We are herein dealing with a multiperforation technique. The cooling zone can be separated in three zones which are usually studied separately: upstream (windward surface), inside the hole and downstream (leeward surface). A good knowledge of the local heat transfer coefficients is necessary to assess the performance of film-cooling. Although the main process is occurring downstream the holes, the heat transfer has also to be determined inside these holes and upstream. A numerical study of the multiperforated plate thermal behaviour [1] puts forward the important contribution of cooling on the windward surface before the air goes through the holes.

This paper presents the results of experimental studies carried out on the windward surface of a multi-perforated flat plate. This study leads to empirical relations which allow the calculation of the heat transfer coefficients as a function of geometric and aerodynamic parameters.

The results obtained by Goldstein and et al. [2] and Sparrow and et al. [3,4] concern the transfer on the back surface of a single perpendicular hole or series of perpendicular holes. Aspiration was performed in a quiet environment or in the presence of a transversal flow. In the case of series of perpendicular holes, the considered spacing is 2 and 2.5 times the hole diameter [4]. The influence of the perforations spacing was not studied, on the one hand this distance is rel-

* Corresponding author. Tel.: +33549498124; fax: +33549498101.
E-mail address: eva.dorignac@let.ensma.fr (E. Dorignac).

1290-0729/$ – see front matter
doi:10.1016/j.ijthermalsci.2004.11.012

Nomenclature

A	active surface	m^2
a	pitch of the in-line perforations repartition	m
d	hole diameter	m
e	thickness of the sample	m
h	local heat transfer coefficient	$W{\cdot}m^{-2}{\cdot}K^{-1}$
$\bar{h}$	average heat transfer coefficient	$W{\cdot}m^{-2}{\cdot}K^{-1}$
$\dot{m}$	air mass flow rate per hole	$kg{\cdot}s^{-1}$
Nu	Nusselt number	
r	distance from perforation axis	m
p	pitch of perforations in staggered rows repartition	m
Pr	Prandtl number	
Re	Reynolds number	
S	hole section surface	m^2
S_h	hexagonal or square section of the symmetric tube upstream the hole	m^2
T	temperature	K
V	air velocity in the hole	$m{\cdot}s^{-1}$
V_h	air velocity upstream hole	$m{\cdot}s^{-1}$
z	distance from the leading edge	m

Greek symbols

ε	emissivity	
φ	heat flux	$W{\cdot}m^{-2}$
λ	thermal conductivity	$W{\cdot}m^{-1}{\cdot}K^{-1}$
ρ	reflectivity of the mirror	

Subscripts

a	relative to the ambient
dissipated	relative to electric power
downstream	relative to flow existing after the perforations
Hole	relative to flow existing inside the perforations
IR	relative to infrared measurements
losses	relative to radiative losses
upstream	relative to flow existing before the perforations
w	relative to the wall

atively short for industrial applications, on the other hand, the perforation diameter is only a few 1/10th millimeter.

Studies about this subject mainly used the technique of heat/mass transfer analogy with naphthalene sublimation [5]. The mean mass transfer coefficient (Sherwood number) and the mean heat transfer coefficient (Nusselt number) by analogy can be worked out by measuring the quantity of naphthalene which diffuses in the air. The disadvantage of this method is that it cannot be used with perforations of small diameters (< 5 mm) because of the probe dimensions used to measure the naphthalene thickness. So, direct measurement of the heat transfer coefficient in the perforations is very difficult for small diameters.

In this paper, we present results obtained from two experimental apparatus. Such experimental studies have the advantage of describing a large number of geometric situations:

- Staggered or in line perforations repartition,
- $1.7 < p/d < 9.7$

for a wide range of Reynolds number, defined as $Re = \frac{Vd}{\nu}$, between 1000 and 12000. The variation of the parameter p/d is obtained either with p varying from 4 to 60 mm, either with d varying from 0.65 to 15 mm. The originality of this work therefore relies on the wide range of variation of the p/d parameter and is related to small diameter perforation cases, usually encountered in real cooling situation.

The study allows us to establish an empirical expression to predict the convective heat transfer in conditions similar to the real ones, but for simplified configurations: perpendicular holes to the wall, aspiration in quiet air.

2. Experimental apparatus

The present experiments were carried out using two experimental devices. One for convective heat transfer at the windward surface of a multi-perforated flat plate whose large diameter (up to 15 mm) holes are in a staggered row position, the other to study convective transfer upstream of a multiperforated plate with a small diameter (around 1 mm) positioned in line.

2.1. Set-up for large diameter perforations

This apparatus allows studying the influence of the following parameters for a repartition in staggered rows:

- Geometric pitch of the multiperforations ($1.7 p/d < 9.6$ with d between 6.25 and 15 mm)
- Velocity of flow (Reynolds number defined with the hole velocity and the hole diameter, $Re = 3000$–8000).

Fig. 1 describes the experimental set-up. A perforated plate is held horizontally at 1.20 m from the ground, below a cubic $1 \times 1 \times 1$ m^3 box. The air is sucked up from the top of the box which allows a homogeneous distribution of the flow through the holes. A thermocouple measures the air temperature before the perforations. The heated surface will thus be horizontal and facing downwards to minimise natural convection effects. The air is sucked up by a fan and through a Venturi linked to a pressure sensor for mass flow measurement.

The experimental principle is to heat up the surface of the perforated plate by a known heat flux. The air flow cools the surface and the measurements are carried out for steady

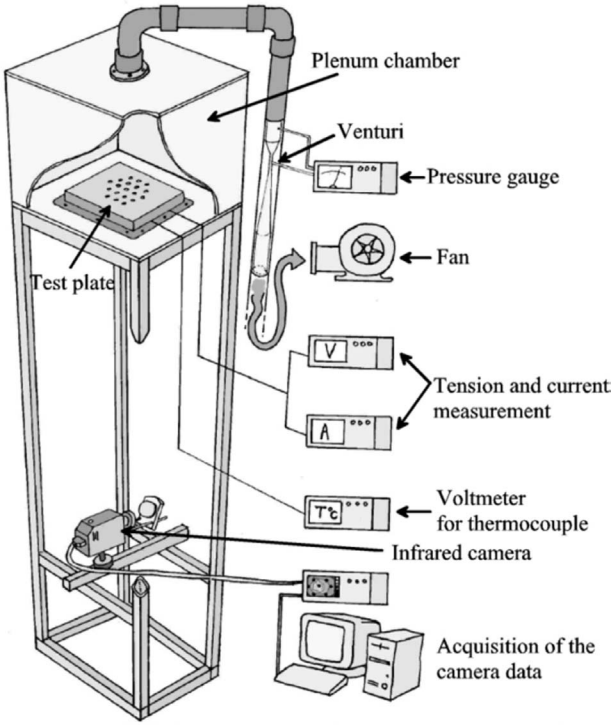

Fig. 1. Set-up sketch.

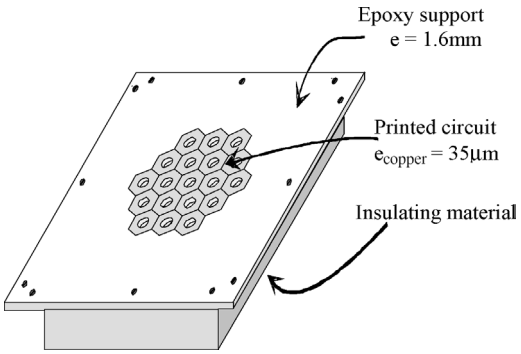

Fig. 2. Drawing of the multiperforated plate and its heating circuit.

flow rates. The perforated test plates (Fig. 2) are made of epoxy with a printed electronic circuit to heat the surface by Joule effect. There is only one copper track which passes around each hole. A layer of an insulating material (conductivity $\lambda = 0.03$ W·m^{-1}·K^{-1}) is stuck on the back surface. Each plate is characterized by the diameter of the holes and the pitch between two holes. A thermocouple probe is located between the back surface of epoxy and the insulation (Fig. 3). It allows for the control of the plate temperature in particular when calculating the emissivity factor of the cooled surface. The heat flux has to be homogeneous around each of the 19 holes. This configuration is complex to obtain and we chose to follow the hexagonal symmetry observed by Sparrow [4] in the design of the printed circuit. An example of such a circuit is presented in Fig. 2 for $p = 2.5$ cm and $d = 1$ cm. It is then painted with high emissivity black paint. The electric power is provided by a regulated D.C. current

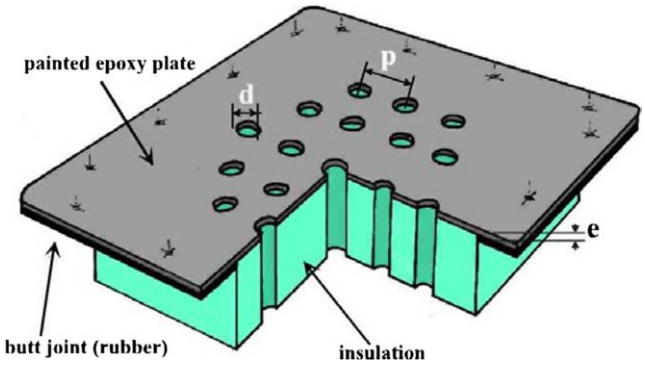

Fig. 3. Geometric parameters.

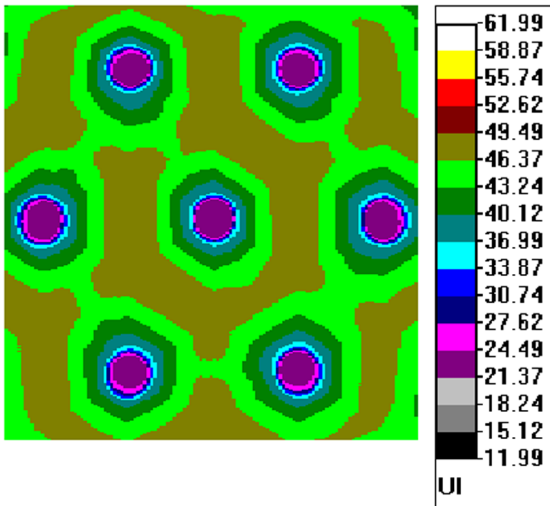

Fig. 4. I.R. Thermograph example.

supply and the tension and current are measured. It is assumed that the totality of this energy is transferred to the air by convection and radiation, and that the conduction through the plate can be neglected.

The camera used is AGEMA 880 SWB, a cryogenically cooled SnSb monodetector camera, a 12° lens, working inside the wavelength range 2.6–5 µm with an accuracy of ±0.5 °C. A series of images (25 per second) is taken for each measurement. With the help of a software program, we use the mean of these images to minimise the influence of noise. As the observed surface is facing the ground, the camera (which has to be horizontal) is installed on a rail under the box and a 45° golden mirror is fixed under the thermal scene (as shown in Fig. 1). Before measurements, the camera has to be adjusted in front of a black body. In the same way, measurements have to be carried out to determine the emissivity value of each plate and the mirror reflectivity value.

The experiments are performed in steady thermal conditions according to the flow rate in the perforations. Five plates are made, instrumented and tested. Infrared thermography is used to access the plate temperature (Fig. 4). As symmetry was observed in that kind of flow [4], we only observe the area of the central hole. The edge effects are minimum here, the significant surface element, called ac-

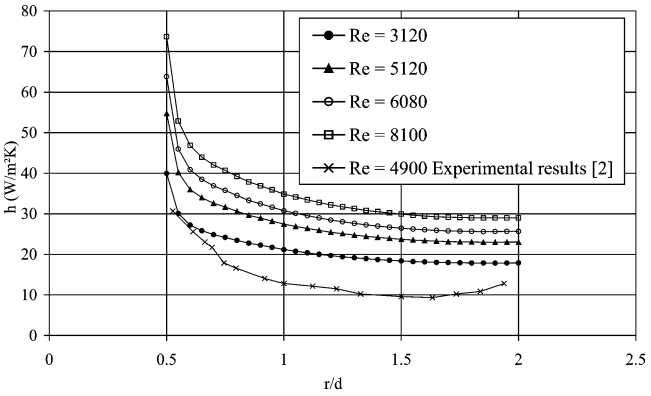

Fig. 5. Local heat transfer coefficient profiles ($p/d = 4$).

tive surface, corresponds to the hexagon (side length: p) minus the hole section. The data allow us to determine radial temperature profiles taking into account the distance to the perforation axe. The emissivity value ($\varepsilon = 0.95 \pm 0.02$) has been previously determined and is also taken into account.

The surface power being precisely known and the part of lost energy by radiation calculated, the local convection heat transfer coefficients are then calculated:

$$h = \frac{\varphi_{\text{dissipated}} - \varphi_{\text{losses}}}{T_w - T_a} \tag{1}$$

where $\varphi_{\text{dissipated}}$ is the electric power dissipated in the plate, and φ_{losses} the radiative losses.

Fig. 5 presents the h variation versus the ratio r/d. The observation of the first millimeters near the perforation ($< 0.004p$) cannot be correctly used by IR thermography because of the spatial resolution limits of the camera. Then, the slope of the local h curve near the hole is certainly exaggerated because of the large gradient between the interior of the hole and its edge. Nevertheless, the acceleration of the air near the inlet of the hole added to the reduction of the thermal boundary layer in this zone leads to a rapid increase of the h value. The shape of this profile is typically the one found in literature [2,4,6]. As we want to obtain the mean convective heat transfer coefficient along the plate, the surface where the heat transfer coefficient value lacks precision being small, it does not influence the mean calculated value. The results of this work are full set of two experiments using tow different techniques, an error calculation leads to a maximum relative error of 6% on the h coefficient average value (confidence level 99%).

2.2. Set-up for small diameter perforations

The direct measurement of the convective heat transfer coefficient is very difficult inside the hole, when its diameter is small. So, we have designed an apparatus which allows for a thermal method of parameters identification. This method is based on a numerical simulation of conductive transfer, associated to measuring wall temperature.

We are then able to study the influence of these parameters for straight line configuration:

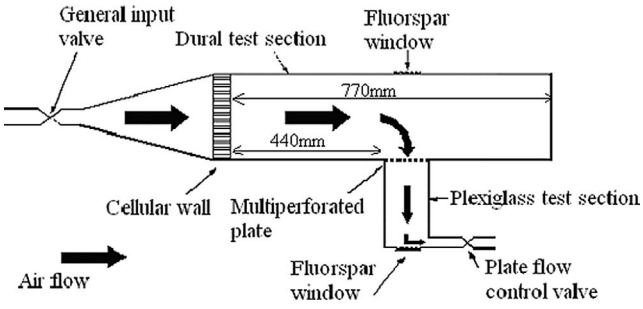

Fig. 6. Sketch of experimental set-up.

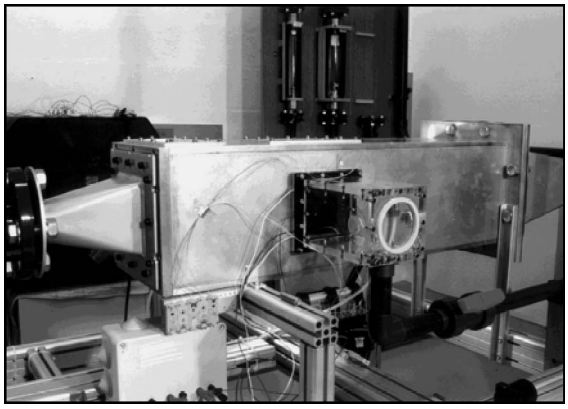

Fig. 7. View of the test section.

- Geometric pitch of the multiperforation ($12.9 < p/d < 9.9$, with d comprised between 0.65 and 2.25 mm),
- Flow velocity (Reynolds number defined with the hole velocity and the hole diameter, $Re = 1000$ to 6000).

The test section (Figs. 6 and 7) has a 190 mm wide square section and is 770 mm long. Air is supplied by centrifugal fan providing a maximal flow rate of 40 g·s^{-1} at the atmospheric pressure. The air is heated at around 10 K above the ambient temperature, by the compression in the fan, so it is necessary to cool it with a heat exchanger to maintain the flow at the ambient temperature. The total mass flow rate is controlled and measured using two standard flow meters (Fischer and Porter). Windows in fluorspar (CaF) allow the measurement of wall temperatures of the multiperforated sample with the infrared camera. The multiperforated sample understudy is placed in a vertical wall of the test section at 440 mm of the inlet (Figs. 6 and 8). The extremity of the plexiglass test section opens on the atmosphere through a valve so that we can regulate the flow rate, its value is measured by a flow meter.

The sample dimensions are 100×100 mm^2 and the usual multiperforated plate is 60×60 mm^2. A numerical study of the multiperforated plate thermal behavior [7] has shown that it is necessary to dissipate energy inside the plate to determine the three heat transfer coefficients involved in this problem. Indeed, in the absence of a dissipated flux inside the wall the plate thermal balance shows that the three heat transfer coefficients involved (upstream, inside

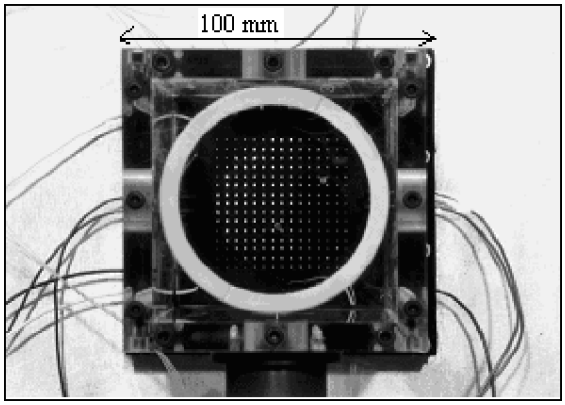

Fig. 8. Multiperforated sample.

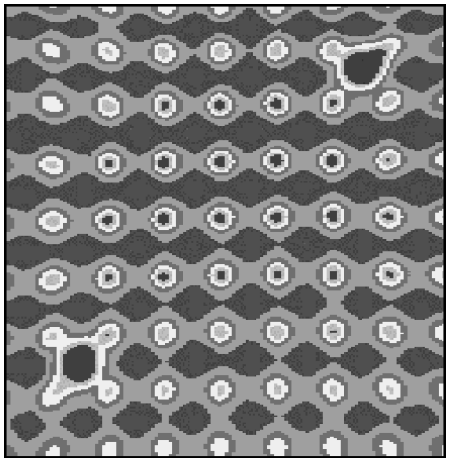

Fig. 9. Example of infrared thermography.

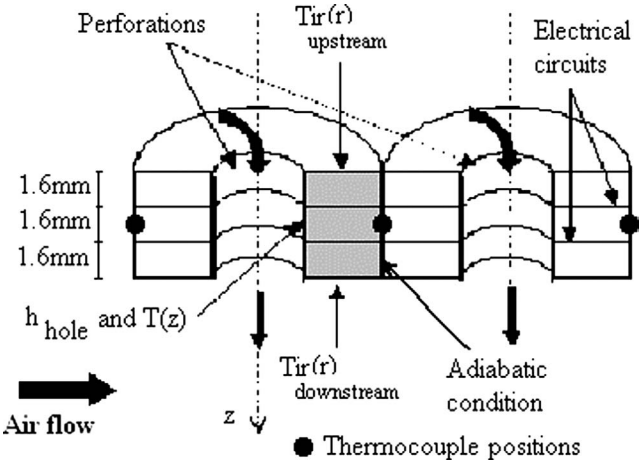

Fig. 10. Localization of axisymmetrical 2D plane.

and downstream the perforations) cannot be determined independently. The sample is then made by assembling three epoxy plates, two with a printed circuit. So, the plate is not heated by the burnt gases as in a combustion chamber but by heat internal dissipation. The epoxy plates are fitted together in such a way that the electrical circuits are positioned at $e/3$ and $2e/3$, where e is the total thickness of the sample. These circuits, made by parallel tracks, are orientated perpendicularly to obtain a regular intersection surrounding the perforations. They are supplied in series to impose the same dissipated power. A third electrical circuit follows the periphery of the sample, and provides a thermal barrier by compensating for a loss of heat by conduction in the test section in Dural®. The upstream and downstream surfaces of the sample are painted in black to give the surfaces the high uniform emissivity required by infrared camera measurements. The emissivity was experimentally estimated at 0.95. The air after going through the perforations sets in the plexiglass test section the exit of which is controlled by a valve. This section is equipped with a fluorspar window to allow infrared measurements. The mass air flow rate going through the multiperforated plate is obtained by the difference between the inlet and the exit flow rate in the section. The measurement of inlet and exit flow rates is carried out with calibration laws of the flow meters at temperature and pressure measured by K type thermocouples and pressure sensors. The air temperature is measured before and after the perforations. Thermocouples are located on the surface of the two sections to allow the necessary correction on radiative fluxes measured by infrared camera on the upstream and downstream sample. On the studied sample, five thermocouples are centered in the thickness and localized on symmetrical planes between perforations (Fig. 10). The electrical supply voltage and intensity are measured to know the local dissipated power in steady state thermal condition. After adjustment of the valves to obtain the requested aerodynamic conditions, the electrical supply imposes a constant heat flux condition at the sample. The imposed constant heat flux is such that, on the one hand the difference of temperature between the plate and the air is sufficient, in the other hand there is no risk of damaging the epoxy plate (that means wall temperature should be less than 70 °C). An experimental verification has shown that the working temperature of the plate has no influence on the coefficients determination. When steady conditions are reached upstream and downstream surface are filmed with an infrared camera. The 100 pictures (25 Hz during 4 s) are averaged to eliminate the measurement noise, so that, an infrared picture is obtained on each face and converted in wall temperature (Fig. 9).

The determination of the convective heat transfer coefficient is carried out using an inverse numerical method from a technique of parameter identification. The simulation of the experiment aims at calculating the temperature which should be measured by thermocouples in the plate for the wall temperatures measured in the experiment and for constant heat coefficient in the holes. The minimization of the gap between the simulated and experimental temperatures gives the value of convective exchange coefficient (h_{hole}) in the perforations. Then, the calculated temperature field in the wall gives the heat fluxes on the upstream and downstream surfaces. Knowing the air temperature upstream and downstream allows calculating the convective exchange coefficient $h_{\text{upstream}}(r)$ and $h_{\text{downstream}}(r)$ leading to the average to obtain h_{upstream} and $h_{\text{downstream}}$. With this experi-

mental technique, we determine a mean value of heat coefficient of the upstream, downstream and inside the perforation area. On the upstream and downstream surfaces, we obtain the distributions corresponding to a simplified model of the exchanges in the perforations (h_{hole} is supposed constant). The developed model is a two-dimensional axisymmetrical model around a central perforation (Fig. 10). The heat internal sources which are the tracks of the printed circuits are modeled by a homogeneous dissipation term on the entire plane of the circuits. The boundary conditions are: h_{hole} and $T_a(z)$ in the hole, $T_{\text{IRupstream}}$ and $T_{\text{IRdownstream}}$ on the upstream and downstream surfaces and an adiabatic condition on the fourth limit which is a symmetric zone between the perforations. The model uses the nodal method [8]. Fig. 11 shows the temperature distribution $T(r,z)$ where $z=0$ is the upstream side, $z=4.8$ mm, the downstream side, $r=0.75$ mm the perforation limit and $z=1.6$ mm and $z=3.2$ mm the electric circuits planes (17.5 μm of thickness). An accuracy estimation has led to a 10% maximum relative error at a 99% confidence level on this mean value of the h coefficient.

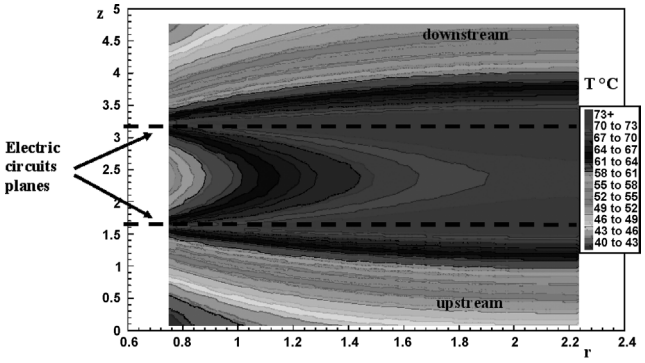

Fig. 11. Example of axisymmetric 2D calculation. Distance r in abscissa and distance z in ordinate.

3. Results

To work out a general correlation for this problem, we have to put together the results with dimensionless numbers (Nusselt number, Reynolds number, aspect ratio) using a relevant reference length and velocity.

The proposed laws in literature [2,4] use a Nusselt number which is based on either the pitch between perforations, or an equivalent diameter. The equivalent diameter is calculated considering an active surface which is the surface of one square pattern minus the hole surface. The work by Sparrow [4] is based on an experimental set-up using the mass transfer method correlation (2) was established for limited variations of the relative spacing between the holes ($p/d=2$ and 2.5):

$$Nu = 0.881 Re^{0.476} Pr^{1/3} \tag{2}$$

with

$$Re = \frac{Vd}{\nu} \tag{3}$$

and

$$Nu = \frac{hA/p}{\lambda} \tag{4}$$

Fig. 12 shows our full set experimental results on compared the Sparrow correlation. Using the Nusselt and Reynolds

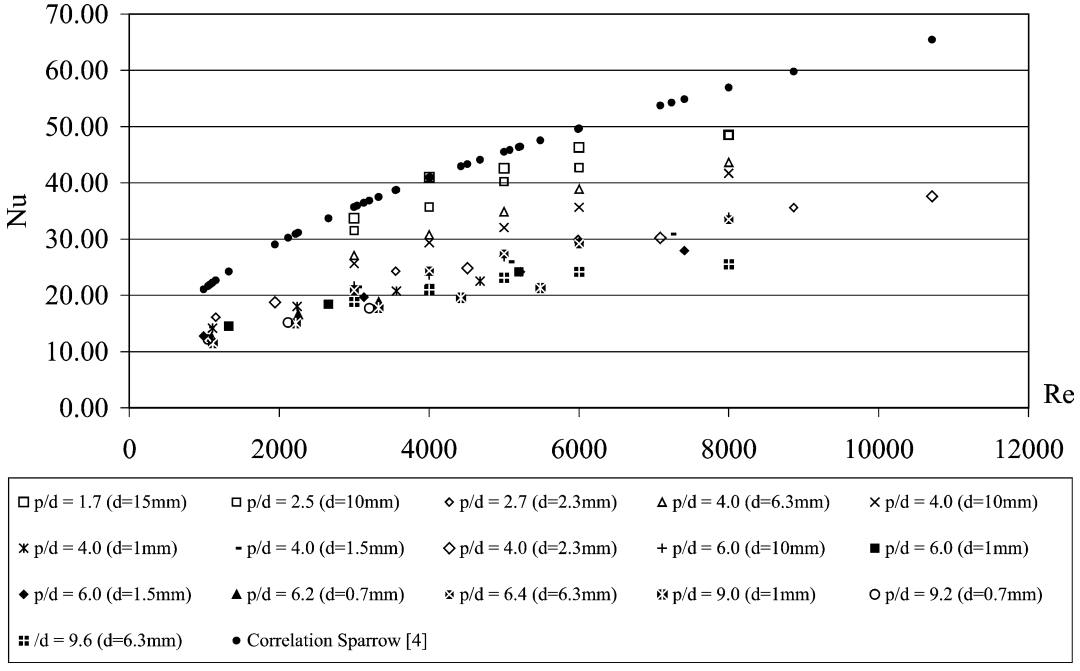

Fig. 12. Experimental points and correlation by Sparrow [4].

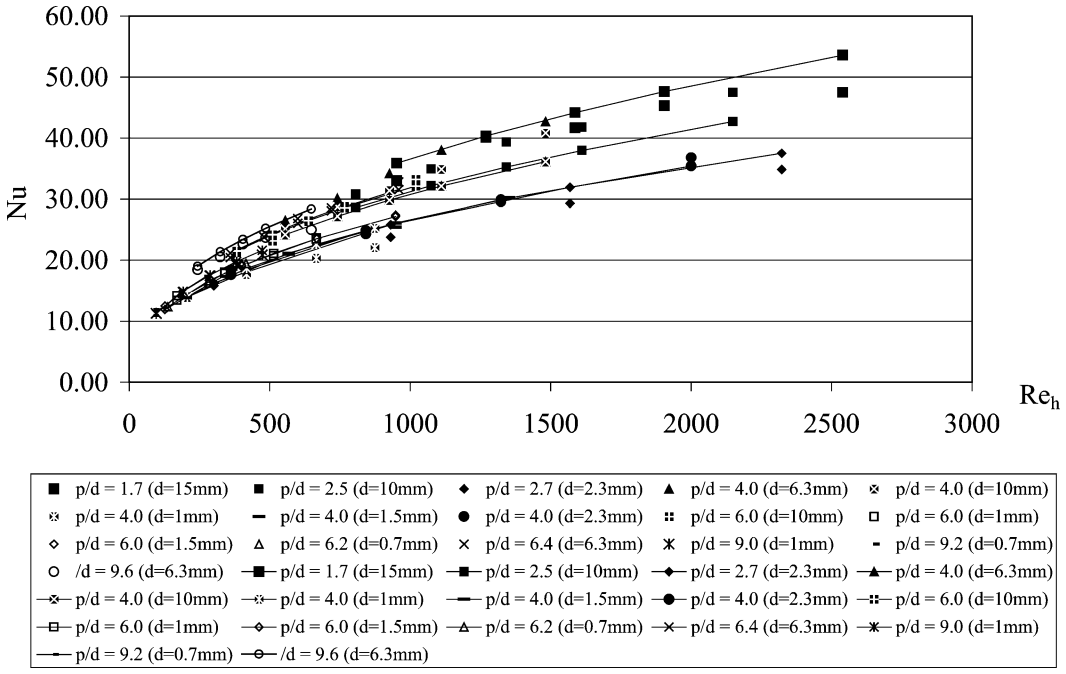

Fig. 13. Comparison of experimental values of the Nusselt number to the ones from proposed correlation (9).

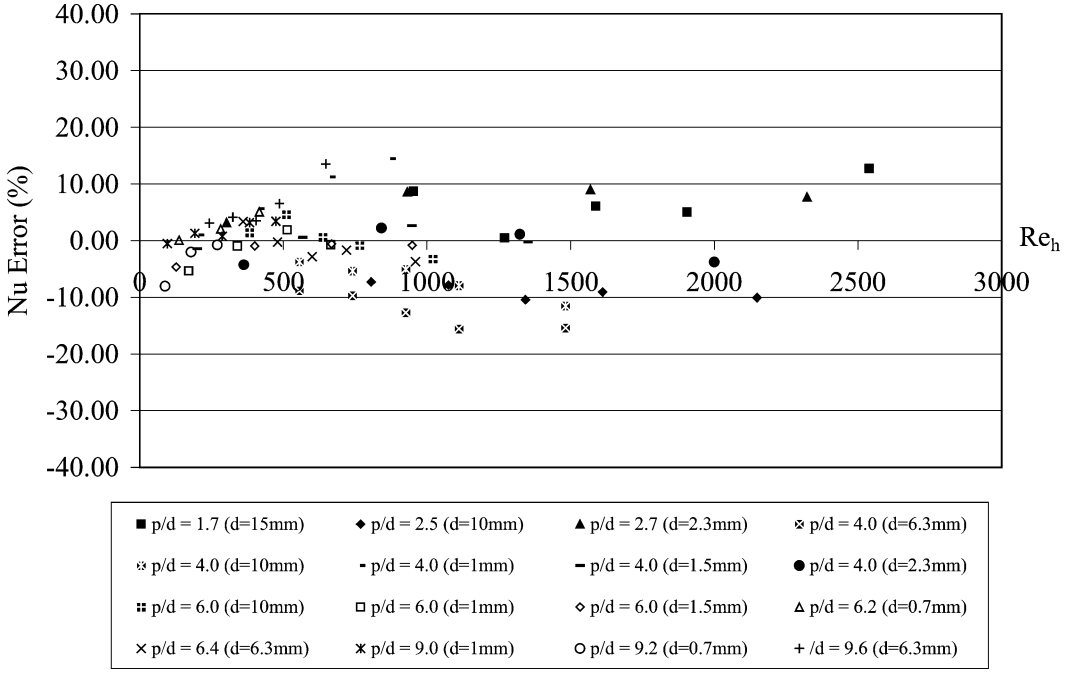

Fig. 14. Gaps between the experimental values and the proposed correlation (9).

numbers defined by (3) and (4). Our results compare quite well with this law since they are close to the experimental case considered by Sparrow ($p/d = 2$ or 2.5) with large perforation diameters. However, when the ratio p/d increases (4, 6, 9) this correlation moves off more and more from the experimental points. Because of the limited range of this correlation, we propose to establish a new correlation which matches all our experimental points.

To establish this correlation, we have taken a different definition of the Reynolds number. Indeed, for a constant Reynolds number, the air velocities on the studied surface vary as a function of the perforations distance. Then, we suppose that the upstream flow goes through a hypothetical tube of either hexagonal section for a staggered row repartition or square section for an in line repartition. The mean velocity in the hole is only linked to the hole diameter and is not representative of the upstream flow. This is

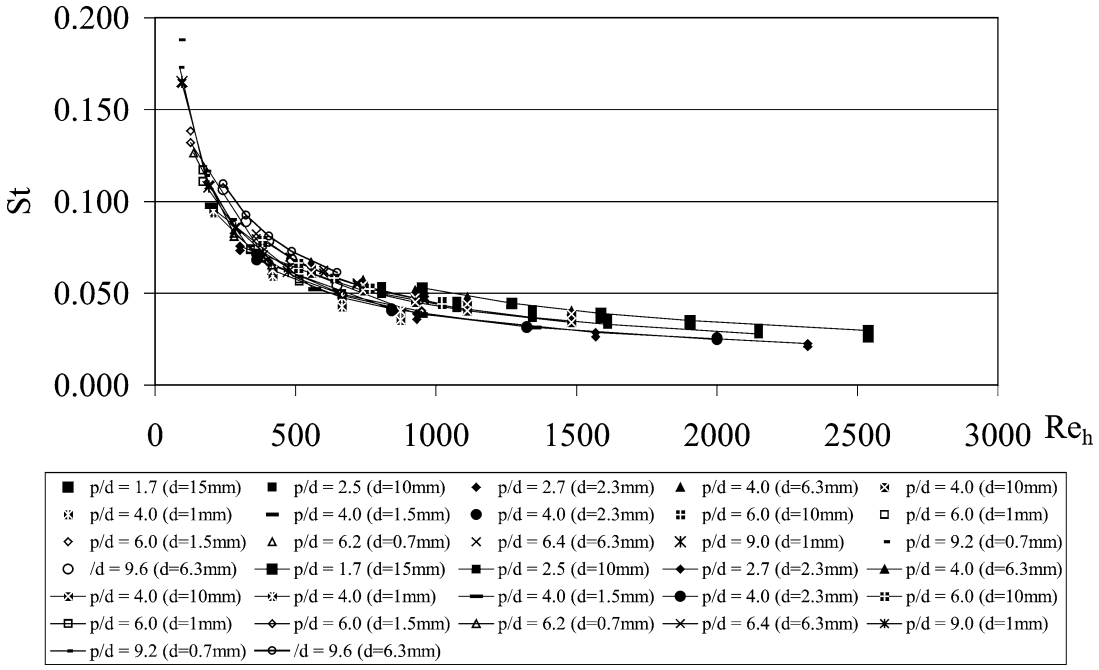

Fig. 15. Comparison of experimental values of Stanton number to those of the proposed correlation (10).

the reason why we define a mean velocity (V_h) from the air mass flow rate per hole and the section of the hypothetical tube:

$$V_h = \frac{\dot{m}}{\rho S_h} \tag{5}$$

with

$$S_h = \frac{3}{2}p^2 \tan\frac{\pi}{6}$$

for staggered row repartition perforations or

$$S_h = a^2$$

for in line repartition perforations.

So, we estimate that it is more relevant to consider the same characteristic length both for the Reynolds number and for the Nusselt number. From the viewpoint of heat transfer, the characteristic length chosen by Sparrow seems to be adapted. This length is the ratio between the active surface (A) whose expression is:

$$A = S_h - \frac{\pi d^2}{4} \tag{6}$$

and the pitch of perforations (p). Then, we propose the following definitions of the Reynolds and Nusselt numbers:

$$Re_h = \frac{V_h A/p}{\nu} \tag{7}$$

$$Nu = \frac{hA/p}{\lambda} \tag{8}$$

All our experimental results do not fit into the introduction of this characteristic length in the numbers without dimension which is classically used. So, we have to take into account two shape factors: one representing the geometric ratio between the active surface and the perforations pitch ($p/\sqrt{A}$), the other one representing the ratio between the pitch and the diameter of the perforations (p/d). Then, we obtain the following relation:

$$Nu = 1.202\left(\frac{p}{\sqrt{A}}\right)^{1,879}\left(\frac{p}{d}\right)^{0,163} Re_h^{0,409} \tag{9}$$

Fig. 13 compares the experimental points (dotted curves) with the points from our correlation, expression (9) (full curves). Fig. 14 shows a good agreement between the experimental points and the one of the correlation plus or minus 15%, and it is noticeable that most points are within a 10% range.

It is also possible to present the results using the Stanton number which has the advantage to be a similarity number instead of the Nusselt number. Correlation (9) then becomes:

$$St = 1.688\left(\frac{p}{\sqrt{A}}\right)^{1,879}\left(\frac{p}{d}\right)^{0,163} Re_h^{-0,591} \tag{10}$$

Fig. 15 presents the variation of this Stanton number for all the experimental cases compared to that obtained by relation (10). This comparison confirms the agreement between the experimental points and the correlation.

4. Conclusion

The results presented in this paper show that convective exchange on the upstream side of a multiperforated plate depends on the pitch between perforations. The laws proposed in the literature, established for a narrow range this parameter do not translate this influence correctly. We have shown

that to calculate the mean convective exchanges around perforations, we must define Nusselt and Reynolds numbers on characteristics (length and velocity) linked to the upstream side and not to the perforations. A law was established for perforations of diameters varying from 0.7 to 15 mm, positioned perpendicularly to the wall and having a staggered row or a in-line repartition with spacing p/d from 1.7 to 9.7. The tested flow rates are characterized by Reynolds number of the upstream flow between 100 to 2500, that corresponds to a Reynolds number between 1000 to 12000 for the perforations flow and velocities between 3 to 90 $\mathrm{m{\cdot}s^{-1}}$ in the perforations.

References

[1] C. Foulon, H. Ledoux, J.J. Vullierme, Etude paramétrique par voie numérique de l'équilibre thermique de la paroi multiperforée d'une chambre de combustion, in: Rencontres S.F.T. 95, 17 au 19/05/95 Poitiers France ed., Elsevier, pp. 611–616.

[2] H.H. Cho, M.Y. Jabbari, J.R. Goldstein, Experimental mass (heat) transfer in and near a circular hole in a flat plate, Internat. J. Heat Mass Transfer 40 (10) (1997) 2431–2443.

[3] E.M. Sparrow, U. Gurdal, Heat transfer at an upstream—facing surface washed by fluid en route to an aperture in the surface, Internat. J. Heat Mass Transfer 24 (5) (1981) 851–857.

[4] E.M. Sparrow, M. Carranco Ortiz, Heat transfer for the upstream face of a perforated plate positioned normal to an oncoming flow, Internat. J. Heat Mass Transfer 25 (1) (1982) 127–135.

[5] R.J. Goldstein, H.H. Cho, Review of mass transfer measurements using naphthalene sublimation, Experimental Thermal Fluid Sci. 10 (1995) 416–434.

[6] G.E. Andrews, M. Alikhanizadeh, F. Bazdini Tehrani, C.I. Hussain, M.S. Koshkbar Azari, Small diameter film cooling holes: The influence of hole size and pitch, ASME Paper N° 87-HT-28, National Heat Transfer Conference, August 1987, Pittsburgh, PA.

[7] C. Foulon, H. Ledoux, J.-J. Vullierme, Etude paramétrique par voie numérique de l'équilibre thermique de la paroi multiperforée d'une chambre de combustion, Congrès SFT 1995, Poitiers.

[8] C. Fort, Estimation de paramètre et méthode inverse en thermique : application à la détermination de la variation du flux pariétal dans une chambre de combustion, Thèse présentée le 22 septembre 1989, Université de Poitiers.